Fusion of Influenza Virus with Cardiolipin Liposomes at Low pH: Mass Action Analysis of Kinetics and Extent†

S. Nir*

The Seagram Center for Soil and Water Sciences, Faculty of Agriculture, The Hebrew University of Jerusalem, Rehovot 76100, Israel

T. Stegmann and J. Wilschut

The Laboratory of Physiological Chemistry, University of Groningen, Bloemsingel 10, 9712 KZ Groningen, The Netherlands

Received April 11, 1985

ABSTRACT: The kinetics and extent of low pH induced fusion between influenza virus and large unilamellar cardiolipin liposomes were investigated with an assay for lipid mixing based on fluorescence resonance energy transfer. The results were analyzed in terms of a mass action kinetic model, which views the overall fusion reaction as a sequence of a second-order process of virus–liposome adhesion or aggregation followed by the first-order fusion reaction itself. The fluorescence development during the course of the fusion process was calculated by numerical integration, employing separate rate constants for the initial aggregation step and for the subsequent fusion reaction. Analytical solutions were found for several limiting cases. Deaggregation of virus–liposome aggregates was explicitly taken into account but was found to be a minor effect under the conditions studied. The calculations gave good simulations and predictions for the kinetics and extent of fusion at different virus/liposome concentrations and ratios. At pH 5.0 and 37 °C, very high rate constants for aggregation and fusion were obtained, and essentially all of the virus particles were involved in the fusion process. Experiments at different virus/liposome ratios showed that fusion products may consist of a single virus particle and several liposomes but not of a single liposome and several virus particles. At pH 6.0, the rate constant for aggregation was the same as at pH 5.0, but the rate constant of fusion was about 5-fold lower, and only 25–40% of the virus particles were capable of fusing with the liposomes. The analytical procedure presented enables elucidation of the crucial role of the composition of target membrane vesicles in the initial adhesion and subsequent fusion of the virus at various pH values.

The infectious entry of influenza virus into cells is thought to consist of the following two major steps. First, after binding to sialic acid containing cell-surface receptors (Carroll et al., 1981; Rogers et al., 1983a,b), the virus particles are internalized by endocytosis through coated pits (Helenius et al., 1980; Matlin et al., 1981; Yoshimura et al., 1982) and routed into the endosomal compartment of the cell (Helenius et al., 1983). Second, induced by the low pH in this compartment (Tycko & Maxfield, 1982; Van Renswoude et al., 1982), the viral membrane fuses "from within" with the membrane of the endosomes, resulting in release of the viral nucleocapsid into the cytoplasm (Helenius et al., 1980; Matlin et al., 1981; White et al., 1983; Tycko & Maxfield, 1982; Marsh et al., 1983). Within the framework of this mechanism, the initial attachment of the virus particles to the target membrane and the subsequent fusion reaction are spaced in terms of both the cellular localization and the stage of the internalization process.

Liposomes (phospholipid vesicles) provide a valuable target membrane system for in vitro characterization of the fusion properties of viruses (Maeda et al., 1981; White & Helenius, 1980; White et al., 1982a). Recently, we have utilized an assay for membrane lipid mixing based on fluorescence resonance energy transfer (RET)[1] (Struck et al., 1981) to study the kinetics of the fusion reaction between influenza virus and liposomes (Stegmann et al., 1985). Fusion was shown to be fast and efficient, and the pH dependence of the process was clearly revealed.

It is important to note that, in contrast to the cellular target membrane of the virus, liposomes composed of phospholipids or phospholipid/cholesterol mixtures lack a specific sialic acid containing receptor. Therefore, the binding of virus particles to liposomes differs from the attachment of the virus to the cellular plasma membrane. Moreover, the nature of the actual fusion reaction with liposomes may be different from the fusion occurring in biological systems. The virus fuses with liposomes of various compositions (Maeda et al., 1981; White et al., 1982a; Stegmann et al., 1985), indicating that the initial virus–liposome interaction is rather nonspecific. However, the kinetics of fusion are strongly dependent on the lipid composition of the liposomes, fusion being most efficient with negatively charged phospholipid vesicles (Stegmann et al., 1985). It is not known whether this preference arises at the level of the initial binding of the virus to the liposomes or at the level of the fusion reaction itself, since the rate of virus–liposome fusion is a composite of the rates of these two steps in the overall process. Furthermore, while it has been shown that the specific, receptor-mediated, attachment of the virus to the cellular plasma membrane is almost independent of the pH (Matlin et al., 1981; Yoshimura et al., 1982), it is not known

† This study was supported in part by the Netherlands Organization for the Advancement of Pure Research (ZWO), National Institutes of Health Grant GM-31506 (Joe Bentz and S.N.), The Hebrew University of Jerusalem (Shainbrun Funds), and EMBO (short-term fellowship to S.N.).

[1] Abbreviations: CL, cardiolipin (bovine heart); HA, hemagglutinin; Hepes, *N*-(2-hydroxyethyl)piperazine-*N*′-2-ethanesulfonic acid; LUV, large unilamellar vesicles; N-NBD-PE, *N*-(7-nitro-2,1,3-benzoxadiazol-4-yl)phosphatidylethanolamine; RET, resonance energy transfer; BHA, bromelain-solubilized hemagglutinin; EDTA, ethylenediaminetetraacetic acid.

0006-2960/86/0425-0257$01.50/0

to what extent the initial kinetics of binding of the virus to liposomes is pH-dependent.

In this paper, we present an analytical procedure, based on a simple mass action kinetic model, which enables one to distinguish between the rate of initial attachment of interacting membrane vesicles and the rate of the subsequent fusion reaction. The model describes the overall process as consisting of a second-order binding step and a subsequent first-order fusion step. Thus, at low particle concentrations the initial binding step is essentially rate-limiting to the process, whereas at higher particle concentrations the fusion reaction per se determines the overall rate to considerable extent. This general model is applied here to evaluate the kinetics of fusion between influenza virus and cardiolipin liposomes, as measured with the RET assay (Stegmann et al., 1985). It is demonstrated that, by performing virus–liposome fusion measurements at different particle concentrations and simulating the data in terms of the model, separate rate constants for virus–liposome binding and for the fusion reaction per se can be obtained. The model developed forms a starting point in the analysis of adherence and fusion phenomena in systems involving liposomes of various compositions or biological membrane vesicles, interacting among themselves, with other target membrane vesicles, or with cells.

Materials and Methods

Lipids. *N*-(Lissamine rhodamine B sulfonyl)phosphatidylethanolamine (N-Rh-PE), *N*-(7-nitro-2,1,3-benzoxadiazol-4-yl)phosphatidylethanolamine (N-NBD-PE), and bovine heart cardiolipin (CL) were obtained from Avanti Polar Lipids, Inc. (Birmingham, AL).

Virus. The X-47 recombinant strain of influenza virus, carrying the hemagglutinin of influenza A/Victoria/3/75, was grown in the allantoic cavity of 10-day–old embryonated eggs and isolated, as described before (Stegmann et al., 1985). The virus was purified by centrifugation for 40 min at 120000*g* in a linear sucrose density gradient (20–60% w/v), containing 10 mM Hepes, pH 7.4. The virus-containing band was isolated, taken to 10% sucrose (w/v) by slow addition of 2.5 mM Hepes, pH 7.4, and stored at −80 °C. Viral phospholipid was determined, after extraction of the membrane lipids (Folch et al., 1957), by phosphate analysis (Bartlett et al., 1959).

Liposomes. Large unilamellar vesicles (LUV), consisting of CL, N-NBD-PE, and N-Rh-PE, were prepared in 150 mM NaCl, 5 mM Hepes, and 0.1 mM EDTA (pH 7.4), as described before (Wilschut et al., 1980). The concentration of the fluorescence probes was 0.6 mol % each, on the basis of lipid phosphorus. The liposomes were sized by extrusion through Unipore polycarbonate filters (Bio-Rad, Richmond, CA) with a pore size of 0.2 μm (Olson et al., 1979). Liposome concentrations were determined by measuring phospholipid phosphorus (Bartlett et al., 1959).

Fusion Assay. Fusion measurements were carried out in a final volume of 1.4 mL, 140 mM NaCl, 10 mM sodium citrate, 10 mM Hepes, and 0.1 mM EDTA, adjusted to the desired pH, essentially as described before (Stegmann et al., 1985). A small volume of virus suspension, appropriately diluted in 147.5 mM NaCl and 2.5 mM Hepes (pH 7.4), was injected into the liposome-containing medium in the cuvette, and the increase of the N-NBD-PE fluorescence, due to dilution of the fluorophores into the viral membrane, was recorded continuously. The medium in the cuvette was stirred magnetically and maintained at 37 °C. Fluorescence was measured in an SLM-8000 fluorometer (SLM/Aminco, Urbana, IL) at excitation and emission wavelengths of 465 and 530 nm, respectively, with a cut-off filter (<515 nm) between sample and emission monochromator. The initial residual fluorescence of the liposomes was taken as the zero intensity and the fluorescence at infinite probe dilution as 100%. The latter value was determined by addition of Triton X-100 (0.5% v/v) to the liposomes and subsequent correction of the fluorescence intensity for the sample dilution and for the effect of Triton on the quantum yield of N-NBD-PE (Struck et al., 1981). It is important to note that, when the initial concentrations of N-NBD-PE and N-Rh-PE in the bilayer are 0.6 mol % each, the fluorescence of N-NBD-PE increases linearly with probe dilution (Struck et al., 1981; Driessen et al., 1985). Furthermore, it has been demonstrated that the fluorophores used in the RET assay do not exchange between membrane vesicles, even under conditions where the vesicles are aggregated (Struck et al., 1981; Hoekstra, 1982; Kumar et al., 1982; Nichols & Pagano, 1983; Rosenberg et al., 1983; Eidelman et al., 1984).

Theory

Mass Action Kinetics of Vesicle–Virus Fusion. The fusion process is viewed as a sequence of two steps: (1) adherence of the virus particles to the liposomes; (2) the fusion process itself, involving destabilization and merging of the membranes (Nir et al., 1980, 1982, 1983; Bentz et al., 1983a,b). The possibility that deaggregation processes may occur is explicitly taken into account. The following notations are used: L and V denote the molar concentrations of liposomes and virus particles, respectively. The molar concentration of an aggregate of I liposomes and J virus particles is denoted by $A(I,J)$. With this notation $L = A(1,0)$ and $V = A(0,1)$. A fusion product consisting of I liposomes and J virus particles will be denoted by $F(I,J)$. We also consider an aggregate formed of any number of liposomes and virus particles attached to any fusion product. Thus, $AF(I_1,J_1,I_2,J_2)$ denotes the concentration of a composite particle consisting of I_1 unfused liposomes, J_1 unfused virus particles, and I_2 liposomes fused with J_2 virus particles. The quantity $FF(I_1,J_1,I_2,J_2)$ denotes the concentration of an aggregation product of $F(I_1,J_1)$ and $F(I_2,J_2)$, i.e., an aggregate of two fusion products, consisting of I_1 liposomes and J_1 virus particles and I_2 liposomes and J_2 virus particles, respectively.

In accord with experimental observations, we do not allow for aggregation-fusion products consisting exclusively of liposomes or virus particles, i.e., $A(I,0) = A(0,J) = F(I,0) = F(0,J) = 0$. Figure 1 illustrates several possible aggregation-fusion products, together with the corresponding reaction pathways. Here we illustrate a few of the initially occurring reactions:

$$\mathrm{L} + \mathrm{V} \underset{D_{11}}{\overset{C_{11}}{\rightleftharpoons}} \mathrm{A}(1,1) \tag{1}$$

$$\mathrm{A}(1,1) \xrightarrow{f_{11}} \mathrm{F}(1,1) \tag{2}$$

$$\mathrm{A}(1,1) + \mathrm{L} \underset{D_{21}}{\overset{C_{21}}{\rightleftharpoons}} \mathrm{A}(2,1) \tag{3}$$

$$\mathrm{A}(1,1) + \mathrm{V} \underset{D_{12}}{\overset{C_{12}}{\rightleftharpoons}} \mathrm{A}(1,2) \tag{4}$$

$$\mathrm{A}(2,1) \xrightarrow{\bar{f}_{11}} \mathrm{AF}(1,0,1,1) \xrightarrow{f_{21}} \mathrm{F}(2,1) \tag{5}$$

The aggregation reaction in eq 1 is of second order, depending on the product of the concentrations L and V. The aggregation rate constants, e.g., C_{11}, C_{21}, ..., C_{IJ} have the units $M^{-1}\,s^{-1}$, whereas the deaggregation rate constants D_{11}, ..., D_{IJ} have the unit s^{-1}. The fusion reactions, eq 2 or 5, are of first order, and the rate constants f_{11}, ..., f_{IJ} have the unit s^{-1}. The

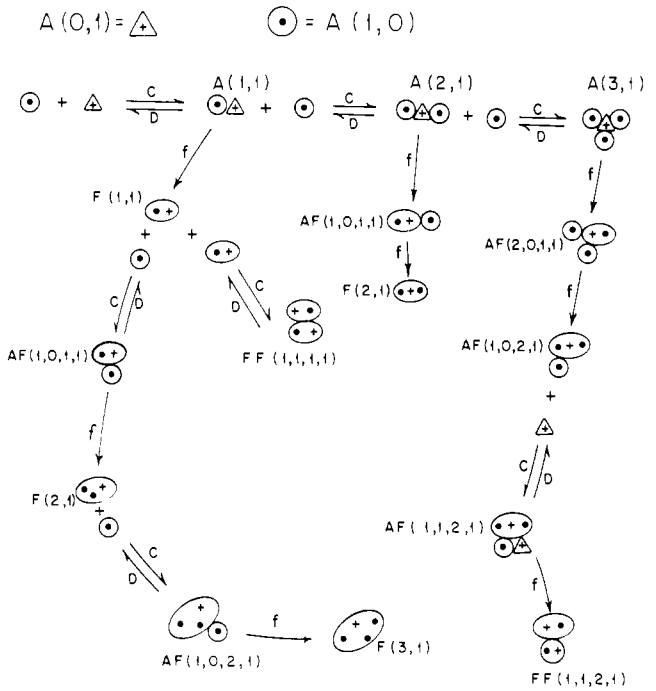

FIGURE 1: An example of several aggregation and fusion products during the initial stages of interaction between influenza virus and liposomes. A virus particle is denoted by A(0,1) and a liposome by A(1,0). For further notations, see Theory.

differential equations describing the kinetics of these reactions are presented in the Appendix. Numerical integration of these equations yields the concentrations of aggregation and fusion products at any stage of the fusion process. In the next paragraph, limiting cases are presented that enable analytical rather than numerical solutions by introducing certain approximations.

Analytical Solutions in Limiting Cases. We will describe analytical solutions for three cases:

(*1*) *Fusion Products Include One Virus Particle and Any Number of Liposomes (Vesicles).* Prior to fusion, the concentrations of vesicles and virus particles are L_0 and V_0, respectively. We consider one rate constant, denoted C, to describe the overall fusion reaction and ignore deaggregation. Strictly, this description pertains to a situation where aggregation is the rate-limiting step of the whole process, but at sufficiently late times every liposome in an aggregate (which contains necessarily a single virus particle) will have fused, and thus, the final results are independent of the ratio between the rate of aggregation and the rate of the fusion per se. For convenience, we denote by $F_1, F_2, ..., F_n$ the concentrations of fusion products consisting of 1, 2, ..., n liposomes corresponding to $F_1 = F(1,1), ..., F_n = F(n,1)$.

Mass conservation of virus particles gives

$$V_0 = V + F_1 + F_2 + ... + F_n \tag{6}$$

The kinetic equations are

$$dL/dt = -CL(V + F_1 + ... + F_n) = -CLV_0 \tag{7}$$

$$dF_1/dt = CLV - CLF_1 \tag{8}$$

$$\vdots$$

$$dF_n/dt = CLF_{n-1} - CLF_n$$

$$dV/dt = -CLV \tag{9}$$

Equation 7 readily gives

$$L(t) = L_0 \exp(-CV_0t) \tag{10}$$

Equations 9 and 10 give

$$V(t) = V_0 \exp\{-(L_0/V_0)[1 - \exp(-CV_0t)]\} \tag{11}$$

Hence, at $t = \infty$ the concentration of unfused virus particles is given by

$$V(\infty) = V_0 \exp(-L_0/V_0) \tag{12}$$

When $L_0 = V_0$, $V(\infty) = V_0 \exp(-1)$, while $L(\infty) = 0$. This result indicates that there is a certain fraction of unfused virus particles, which depends on the ratio L_0/V_0 and is explained by the fact that each fusion product can include just a single virus particle but any number of liposomes.

At initial times, such that $CV_0t \ll 1$, eq 10 becomes

$$L(t) = L_0(1 - CV_0t) \tag{13}$$

or

$$L_0 - L(t) = CL_0V_0t \tag{14}$$

or

$$[L_0 - L(t)]/L_0 = CV_0t \tag{15}$$

Hence, at short times the fraction of fused vesicles is increasing linearly with time as well as with the concentration of virus particles. Initially, multiple fusion events can be neglected, implying that eq 14 also gives the concentration of fused virus particles:

$$V_0 - V(t) = CL_0V_0t \tag{16}$$

or

$$[V_0 - V(t)]/V_0 = CL_0t \tag{17}$$

Hence, at short times the fraction of fused virus particles is proportional to the concentration of liposomes. Equation 16 can be also obtained as a limiting case of eq 11.

(*2*) *Fusion Products Include a Single Vesicle and Any Number of Virus Particles.* An interchange between the letters L and V in eq 10 and 11 yields

$$V(t) = V_0 \exp(-CL_0t) \tag{18}$$

$$L(t) = L_0 \exp\{-(V_0/L_0)[1 - \exp(-CL_0t)]\} \tag{19}$$

At $t = \infty$, the concentration of unfused liposomes is

$$L(\infty) = L_0 \exp(-V_0/L_0) \tag{20}$$

At short times the results are necessarily the same as those in eq 13–17.

(*3*) *Fusion Products Consist of a Single Vesicle and a Single Virus Particle.* Here, we distinguish between the aggregated dimer denoted by A and a fused doublet denoted by F. The mass conservation relations are

$$L_0 = L + A + F \tag{21}$$

and

$$V_0 = V + A + F \tag{22}$$

The kinetic equations are

$$dL/dt = -CLV \tag{23}$$

$$dA/dt = CLV - fA \tag{24}$$

$$dF/dt = fA \tag{25}$$

Hence, we distinguish between C, the rate constant of aggregation or adhesion, and f, the rate constant of fusion.

The substitution of V from eq 22 into eq 23 yields

$$dL/dt = -CL(V_0 - A - F) \tag{26}$$

and substituting $A + F$ from eq 21 into eq 26 gives

$$dL/dt = -CL(V_0 - L_0 + L) = -C[L^2 + L(V_0 - L_0)] \tag{27}$$

When $L_0 \neq V_0$, the solution for L is

$$L(t) = (QL_0/V_0)/[L_0/V_0 - \exp(-CQt)] \tag{28}$$

in which $Q = L_0 - V_0$. When $L_0 = V_0$, the solution for L is

$$L(t) = L_0/(1 + CL_0t) \quad (29)$$

The solution for F is readily obtained, albeit in an implicit form

$$F(t) = f \exp(-ft) \int [L_0 - L(S)] \exp(fS)\, dS \quad (30)$$

in which L is taken from eq 28 or 29.

At very long times, eq 28 and 29 show that

$$L(\infty) = L_0 - V_0 \quad (31)$$

if $L_0 > V_0$ and

$$L(\infty) = 0$$

otherwise. When it is assumed that adhesion is rate-limiting to the overall fusion process, i.e., $f \gg CL_0$, the solution is simply given by

$$F(t) = L_0 - L(t) \quad (32)$$

where $L(t)$ is given by eq 28 or 29. At short times, there is again a linear increase of $F(t)$ with time and with virus concentration, as given by eq 15.

It may be emphasized that in case 2 no unfused virus particles or liposomes remain after long times in a 1:1 mixture, and the concentration of the component in excess is reduced by an amount equal to the initial concentration of the other component. In contrast, in case 1 no unfused liposomes will remain even if they are in excess, whereas there will remain unfused virus particles at a final concentration that depends on the ratio V_0/L_0. At short times the concentration of fusion products increases linearly with time and with the product of the concentrations of the components, provided that adhesion is rate-limiting to the overall fusion process. Such a condition can be attained by diluting the concentrations of the components so that the relation $L_0C \ll f$ is satisfied.

Final Levels of N-NBD-PE Fluorescence. The approximate analytical solutions can readily provide the final levels of N-NBD-PE fluorescence. In the linear regime, i.e., at surface probe concentrations of 0.6 mol % or less (Struck et al., 1981), the percent increase in fluorescence intensity per N-NBD-PE molecule, y, depends on the surface probe concentrations, according to

$$y = 100(1 - x) \quad (33)$$

in which x is probe concentration relative to the initial value. At infinite dilution $x = 0$ and $y = 100$, whereas initially $x = 1$ and $y = 0$. Now, let % Fl be the intensity increase due to the dilution of the probes upon fusion of labeled liposomes within virus particles of the same size, and let N denote the average number of fused virus particles per fused liposome. The unfused liposomes do not contribute to the fluorescence increase. The average value of x in eq 33 is $1/(N + 1)$. Since the relative concentration of fused liposomes is $[L_0 - L(\infty)]/L_0$, we have

$$\% \text{ Fl} = 100[L_0 - L(\infty)]N/[L_0(N + 1)] \quad (34)$$

For instance, if $L(\infty) = L_0$, i.e., no fusion has occurred, % Fl = 0; if $L(\infty) = 0$ in a 1:1 mixture where $N = 1$, then % Fl = 50; if $L(\infty) = 0$ in a 1:2 mixture where all virus particles have fused, then $N = 2$ and % Fl = 66.7; in a 2:1 mixture where only one virus particle fuses per liposome, then $L(\infty) = L_0/2$, $N = (L_0/2)/[L_0 - L(\infty)] = 1$, and % Fl = 25.

If x in eq 34 is not given by $1/(N + 1)$ but, say, by $1/(Nd + 1)$, then eq 34 is generalized to

$$\% \text{ Fl} = 100Nd[L_0 - L(\infty)]/[(Nd + 1)L_0] \quad (35)$$

The case $d \neq 1$ can arise because of a difference in the sizes of vesicles and virus particles and can also represent certain constraints, such as deviations from homogeneous probe distribution in the fusion products.

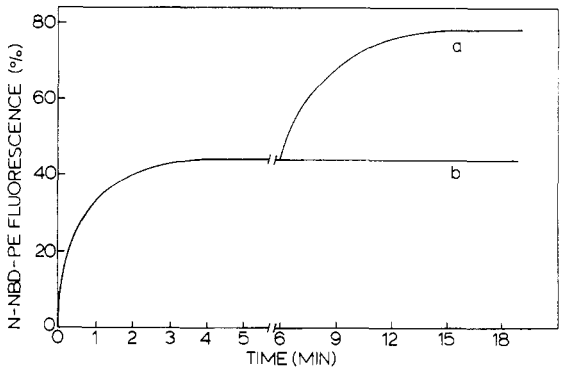

FIGURE 2: Continued fusion of virus–liposome fusion products with liposomes, but not with virus. Influenza virus and fluorescently labeled CL liposomes were fused at pH 5.0 and 37 °C at concentrations of 25 μM lipid phosphorus each. After 6 min, additional nonlabeled liposomes (curve a) or virus particles (curve b) were added to yield final virus/liposome ratios of 1:4 and 4:1, respectively.

Results

Table I presents the final levels of N-NBD-PE fluorescence intensity observed after long incubation (>1 h) of influenza virus with fluorescently labeled CL liposomes at different ratios, under optimal conditions for fusion, i.e., at a temperature of 37 °C and pH 5.0. Table I also shows values calculated by three types of analytical solutions and values calculated by assuming a homogeneous mixture of all membrane lipids in the system. Comparison between the experimental and calculated fluorescence levels indicates that the experimental results are close to the values given by an analytical solution that allows for fusion products consisting of any number of liposomes fused with a single virus particle but prohibits the fusion of an additional virus particle with the fusion products.

The conclusion emerging from the results in Table I was confirmed by the experiment shown in Figure 2. Virus and labeled CL liposomes were fused at pH 5.0 at a 1:1 ratio. Subsequently, when the final level of N-NBD-PE fluorescence was attained, additional nonlabeled liposomes or virus particles were added to yield final virus/liposome ratios of 1:4 and 4:1, respectively. When additional liposomes were added, a further increase in fluorescence was observed (Figure 2, curve a), indicating fusion between the liposomes and the initially formed fusion products. By contrast, additional virus did not produce any further increase in fluorescence, showing that the virus did not fuse with the fusion products. The results in Table I and Figure 2 can be summarized by stating that at pH 5.0 and 37 °C all virus particles are active, and the fusion products consist of a single virus and one or more liposomes.

Information about the overall fusion rate and about the rate constants was obtained by an analysis of the kinetics of fluorescence increase. Figure 3 and Table II illustrate the kinetics of fusion for mixtures containing equal concentrations of virus particles and liposomes. The total lipid concentration was varied between 1 and 50 μM (lipid phosphorus). The results show that the overall rate of fusion increases with increasing lipid concentration. At the initial stages, the fluorescence increases linearly with lipid concentration and with time, in accord with eq 17.

The results in Figure 3 and Table II demonstrate that the kinetics of fusion are well simulated by the calculations over a wide range of incubation times and concentrations. The

Table I: Final Levels of N-NBD-PE Fluorescence (%) at pH 5.0

ratio of liposomes:virus (lipid phosphorus)	calcd for fusion products consisting of: a homogeneous mixture of liposomal and viral lipid	a single liposome and a single virus particle	a single liposome and any number of virus particles	a single virus particle and any number of liposomes	exptl values[a]: batch 1	batch 2
16:1	5.9	3.1	3.1	5.9	5.3	4.3
8:1	11.1	6.2	6.1	11.1	11.0	11.0
4:1	20.0	12.5	11.7	19.7	20.0	21.0
2:1	33.3	25.0	22.0	30.2	28.0	33.0
1:1	50.0	50.0	38.7	38.7	37.0	44.0
1:2	66.6	50.0	60.4	44.0	41.0	46.0
1:4	80.0	50.0	78.8	46.9		47.0
1:8	89.0	50.0	89.0	48.4		48.0
1:16	94.0	50.0	94.0	49.2		49.0

[a] Values for two different batches of virus are shown. T = 37 °C.

Table II: Kinetics of Fusion of Influenza Virus with Cardiolipin Liposomes at pH 5.0: A Comparison between Experimental and Calculated Values of N-NBD-PE Fluorescence (%)[a]

time (s)	ratio of virus:liposomes (lipid phosphorus) 1:1 exptl	1:1 calcd	1:2 exptl	1:2 calcd	1:8 exptl	1:8 calcd
1.2	2.7	2.6	2.4	1.4	0.9	0.4
2.4	5.9	6.9	4.3	3.8	1.8	1.0
6.0	13.2	16.9	9.3	10.2	3.4	3.0
18.0	26.0	28.3	18.6	19.5	6.3	6.4
30.0	30.5	31.9	22.4	23.1	7.4	7.8
60.0	34.2	35.6	26.0	27.0	8.3	8.9

[a] The concentration of CL liposomes was 25 μM (lipid phosphorus). The results for virus:liposomes ratios of 2:1, 1:1, 1:4, and 1:16 are given in Figure 5. The calculations employed the rate constants $C = 4.3 \times 10^8$ M^{-1} s^{-1}, $f = 0.9$ s^{-1}, and $D = 0.025$ s^{-1}. T = 37 °C.

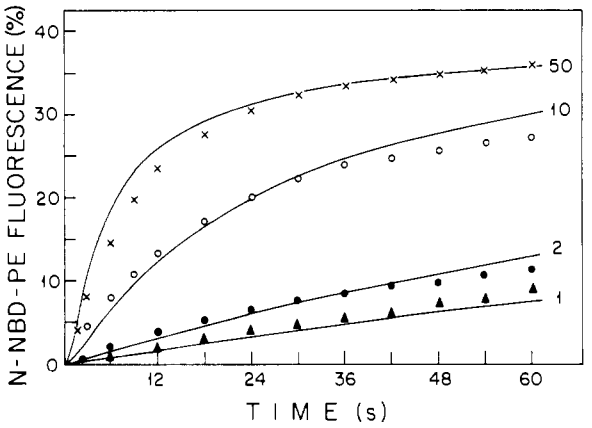

FIGURE 3: Kinetics of N-NBD-PE fluorescence increase during fusion of influenza virus with CL liposomes at 37 °C and pH 5.0. Virus:liposome ratio (based on lipid phosphorus) was 1:1. Total micromolar lipid phosphorus concentrations are indicated. Experimental values are given by data points, and calculated values are given by the drawn lines. Rate constants employed were $C = 5 \times 10^8$ M^{-1} s^{-1}, $f = 1.1$ s^{-1}, and $D = 0.025$ s^{-1}.

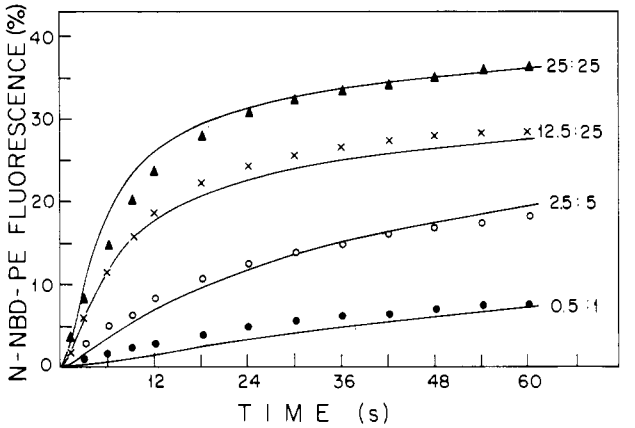

FIGURE 4: Kinetics of N-NBD-PE fluorescence increase during fusion of influenza virus with CL liposomes at 37 °C and pH 5.0. The numbers indicated represent the ratios of micromolar viral to liposomal lipid phosphorus concentrations. Experimental values are given by data points, and calculated values are given by the drawn lines. Rate constants employed were $C = 5 \times 10^8$ M^{-1} s^{-1}, $f = 1.1$ s^{-1}, and $D = 0.025$ s^{-1}.

simulation of the kinetics of fluorescence increase was achieved by employing two parameters, the rate constant of aggregation, or adhesion, C, (M^{-1} s^{-1}), and the rate constant of fusion per se, f (s^{-1}). Following the conclusion drawn from the analysis of final levels of fluorescence, the calculations did not allow for the fusion of a virus particle with a fusion product. In the first stage of the analysis, the rate constant of aggregation, C, was determined from the results on a 1:1 virus–liposome mixture at a low lipid concentration. Thus, the condition $L_0C \ll f$ was satisfied, implying that in this case fusion followed the attachment of a virus particle to a liposome with no appreciable delay. The results obtained with suspensions of low lipid concentrations are relatively insensitive to f values (provided that the condition $L_0C \ll f$ holds) and could, therefore, also be simulated by the analytical solution, shown in eq 18 and 19. After having fixed the value of C, we determined the value of f, the rate constant of fusion per se, by simulating the results of fusion kinetics in more concentrated suspensions with the numerical solutions presented in the Appendix. The process of deaggregation of virus–liposome aggregates was considered explicitly. Particularly at the later stages of the fusion process, the fluorescence results become increasingly sensitive to deaggregation. However, we found an optimal simulation of the data by setting the rate constant for deaggregation, D, close to zero.

Having determined the two parameters C and f from the results on 1:1 mixtures, we were able to make predictions for the kinetics of fluorescence increase in other mixtures. Figure 4 illustrates the kinetics of fusion for several samples in which the ratio between virus particles and liposomes was 1:2. Figure

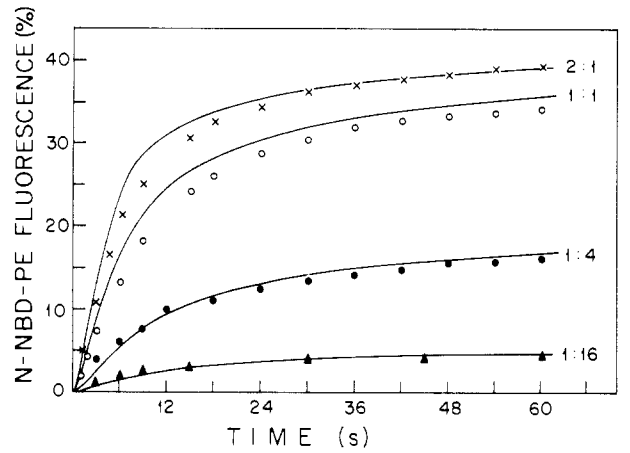

FIGURE 5: Kinetics of N-NBD-PE fluorescence during fusion of influenza virus and CL liposomes at 37 °C and pH 5.0. The liposome concentration was 25 μM (lipid phosphorus) while the ratio of virus to liposomes (based on lipid phosphorus) was varied, as indicated. Experimental values are given by data points, and calculated values are given by the drawn lines. Rate constants employed were $C = 4.3 \times 10^8$ M^{-1} s^{-1}, $f = 0.9$ s^{-1}, and $D = 0.025$ s^{-1}.

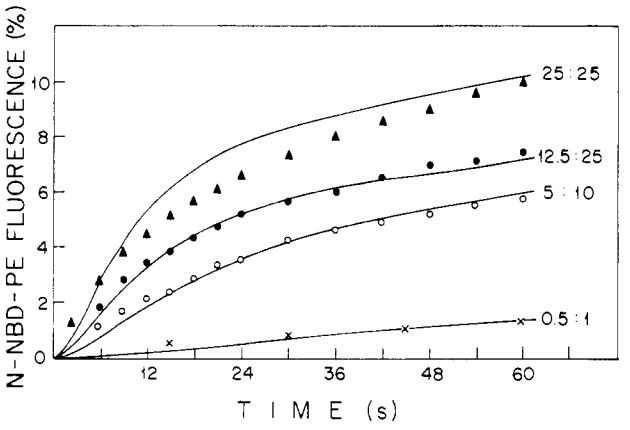

FIGURE 6: Kinetics of N-NBD-PE fluorescence increase during fusion of influenza virus with CL liposomes at 37 °C and pH 6.0. The numbers indicated represent the ratios of micromolar viral to liposomal lipid phosphorus concentrations. Experimental values are given by data points, and calculated values are given by the drawn lines. Rate constants employed were $C = 4.3 \times 10^8$ M^{-1} s^{-1}, $f = 0.25$ s^{-1}, and $D = 0.025$ s^{-1}. In the calculations it was assumed that 75% of the virus particles were unable to fuse with the liposomes (Table III). The inactive virus was allowed to bind to the liposomes, but fusion was prohibited.

Table III: Final Levels of N-NBD-PE Fluorescence at pH 6.0

ratio of liposomes:virus (lipid phosphorus)	calcd[a] for active virus particles (%)			
	100	50	25	exptl
1:1	38.7	30.2	19.7	18.1
2:1	30.2	19.7	11.1	14.9

[a] The calculations assumed that fusion products consisted of a single virus particle and any number of liposomes. $T = 37$ °C.

5 illustrates the effect of varying the ratio between liposomes and virus particles. Figures 4 and 5 demonstrate enhancement in the overall rate of fluorescence increase as the ratio of virus to liposomes increases.

At pH 6.0 the final fluorescence levels were lower than in the corresponding cases at pH 5.0. Table III indicates that the final levels can be explained by assuming that the fraction of active virus particles was between 0.25 and 0.4. The overall kinetics of fusion were significantly slower than at pH 5.0 (Figure 6). Part of this retardation is due to the presence

Table IV: Rate Constants Describing Kinetics of Fusion of Influenza Virus with Cardiolipin Liposomes at pH 5.0 and pH 6.0[a]

pH	aggregation rate constant, C (M^{-1} s^{-1})	fusion rate constant, f (s^{-1})	deaggregation rate constant, D (s^{-1})
5.0	4.3×10^8	0.9	0.025
5.0	5.0×10^8	1.1	0.025
5.0	10^9	1.7	0.025
6.0	4.3×10^8	0.25	0.025

[a] The estimated uncertainties in C values are 10–20%; the uncertainties in f and D values are 20–30% and approximately 50%, respectively. The different results at pH 5.0 reflect the variability between different virus batches. $T = 37$ °C.

Table V: Distribution of Aggregation-Fusion Products in 1:1 Mixtures[a]

	lipid concn (μM)[b] at $T = 6$ s		lipid concn (μM)[b] at $T = 12$ s	
	50	1	50	1
% fluorescence	16.9	0.6	24.7	1.3
% fused liposomes	38.0	1.2	59.4	2.7
% fused virus	31.8	1.2	44.9	2.7
% A(1,0)	49	98	28	97
% A(0,1)	49	98	29	97
% A(1,1)	4	0.3	1.4	0.26
% A(2,1)	0.3	7×10^{-4}	0.1	7×10^{-4}
% A(3,1)	0.03	2×10^{-6}	0.01	2×10^{-6}
% A(4,4)	4×10^{-3}	0	1.2×10^{-2}	0
% F(1,1)	18	1.1	17	2.6
% F(2,1)	3.6	0.07	6	0.3
% F(3,1)	0.6	3×10^{-5}	2	3×10^{-4}
% AF(1,0,1,1)	1.4	3×10^{-3}	0.84	7×10^{-3}
% AF(1,1,1,1)	1.1	7×10^{-5}	1.7	4×10^{-4}
% AF(2,0,1,1)	0.13	9×10^{-6}	0.06	2×10^{-5}
% AF(2,2,1,1)	0.12	5×10^{-9}	0.30	8×10^{-8}
% FF(1,1,1,1)	0.5	3×10^{-7}	1.6	3×10^{-4}
% FF(2,1,1,1)	0.08	10^{-9}	0.4	3×10^{-6}

[a] The percent fused liposomes is given by $(100/L_0)\sum[IF(I,J) + I_2AF(I_1,J_1,I_2,J_2) + (I_1 + I_2)FF(I_1,J_1,I_2,J_2)]$. A similar expression is obtained for the percent fused virus particles. The calculations employed the rate constants $C = 4.3 \times 10^8$ M^{-1} s^{-1}, $f = 0.9$ s^{-1}, and $D = 0.025$ s^{-1}. The numbers opposite A(1,0), F(1,1), etc. represent the percent of the number of particles of those aggregation-fusion products relative to the initial number of liposomes. Note that the percent of liposomal lipid in the fusion product F(2,1) or F(3,1) is 2 or 3 times the value of these products, respectively. [b] The concentrations of liposomes and virus particles are 25 or 0.5 μM, on the basis of lipid phosphorus.

of a considerable fraction of inactive virus particles. In addition, for the active virus the rate constant for the fusion reaction per se was considerably smaller than at pH 5.0. By contrast, the rate constant for the aggregation step was the same as that at pH 5.0. In the analysis of the data at pH 6.0, a third species, i.e., the inactive virus particle, was introduced in the program. This particle was allowed to adhere to the liposomes with the same aggregation rate constant as that for the active virus particles. However, fusion was prohibited, and the rate constant for deaggregation was set to the same low value as that at pH 5.0 for all aggregates.

Table IV presents a summary of the rate constants, C, f, and D, that gave an optimal agreement between calculated and experimental values. Table V illustrates the distribution of aggregation-fusion products for two lipid concentrations in a 1:1 mixture of the virus and the liposomes (pH 5.0) at two incubation times. In the more dilute lipid suspension (1 μM total phospholipid), the aggregation is rate-limiting to the overall fusion process. In this case, the condition $f \gg CL_0$ holds; $f = 0.9$ s^{-1} whereas $CL_0 = 1.5 \times 10^{-3}$ s^{-1}. At $t = 6$ s, the ratios $F(1,1)/A(2,1)$ equal 1500 and 60 for $L_0 = 0.5$ and 25 μM, respectively. These numbers illustrate the statement

that in the limit $f >> CL_0$ aggregation is the rate-limiting step, and once aggregates are formed, fusion occurs almost instantaneously.

The results with the more dilute suspension indicate an approximate linear increase of the percent fluorescence with time. In this case, the percent fused liposomes is close to twice the percent fluorescence and equals the percent fused virus particles. When $L_0 = 25$ μM, the aggregation-fusion reaction has reached a more advanced stage, at which the percent fused liposomes is more than twice the percent fluorescence, whereas the percent fused virus particles is smaller. This difference arises because the calculations considered the fusion products to consist of several liposomes and a single virus particle. Thus, at later stages the observed percent fluorescence only gives an approximate estimate of the percent fused virus particles. Initially, when the percent fused particles is small, say, below 10 (or the percent fluorescence < 5), most of the fusion products are accounted for by fused doublets, $F(1,1)$, which consist of one liposome and one virus particle. However, when the percent fused liposomes is 38, only 18% of the liposomes are in fused doublets, and their relative weight further decreases as the aggregation-fusion reaction proceeds (Table V).

Discussion

In this study a mass action kinetic model is applied, for the first time, to the analysis of the fusion properties of a biological membrane, i.e., the membrane of influenza virus. The model views the overall fusion reaction as a sequence of a second-order process of aggregation or adhesion between interacting membrane vesicles followed by the first-order fusion reaction itself. The kinetics of the pH-dependent fusion between influenza virus and unilamellar CL vesicles, as measured with the RET assay (Struck et al., 1981; Stegmann et al., 1985), could be well simulated and predicted by the model.

The number of adjustable parameters in the model has been limited to a minimum. No parameters are required for the calculation of the final extents of fusion (Table I). The analysis of the initial fusion kinetics, in general, requires two parameters, the rate constant of aggregation, C, and the rate constant of the actual fusion, f. When low lipid concentrations are employed, the aggregation is rate-limiting to the overall fusion process, and the results could be simulated by employing just the parameter C. In this case, the numerical integration could be replaced by the more simple analytical solution given in eq 10 and 11. At higher lipid concentrations, where the fusion reaction itself determines to a considerable extent the rate of the overall process, both C and f had to be employed, and the fluorescence was calculated by numerical integration. In principle, another parameter, the rate constant for deaggregation has to be taken into account as well. However, it turned out that the results could be best simulated by setting its value close to zero (Table IV). By employing just one value for each of the parameters C and f, we do not intend to suggest that the rates of aggregation and fusion during the initial dimerization are the same as those during the formation of higher order aggregation and fusion products. The analysis is most sensitive to the initial stage of the process, and it is difficult to determine changes in the rate constants at later stages.

At pH 5.0 and 37 °C, fusion of influenza virus with CL liposomes is fast, and essentially all of the virus particles are involved in the fusion process (Table I). Under these conditions, the aggregation rate constant [$(4–10) \times 10^8$ M^{-1} s^{-1}] is very large, just 1 order of magnitude below its value in diffusion-controlled aggregation (Smoluchowski, 1917). This means that there is hardly any potential energy barrier for adhesion of a virus particle to a CL liposome, i.e., most of the collisions result in the formation of stable aggregates. Furthermore, the adhesion is essentially irreversible (Table IV). Preliminary analyses have shown that, as expected for irreversible adhesion (Nir et al., 1980b), the aggregation rate constant decreases when the temperature is lowered (unpublished results). The rate constant for the actual fusion reaction at pH 5.0 ($1–2$ s^{-1}, Table IV) is comparable to, for example, fusion rate constants obtained for the Ca^{2+}-induced fusion of CL-containing vesicles among themselves (Wilschut et al., 1985). The value of $1–2$ s^{-1} implies that, starting from a hypothetical condition in which all virus particles are present as aggregated dimers consisting of one virus particle and one CL liposome, 10% of the virus will be fused after 100 ms and 63% after 1 s.

The results in Table I show that at the ratios of virus to liposomes employed the fusion products may consist of a single virus particle and several liposomes. This result implies that fusion products do have the capacity to fuse with nonfused liposomes but not with nonfused virus particles or other fusion products (Figure 2). The reason for this lack of fusion remains unclear but is presumably related to mutual interference of the viral spike glycoproteins, determined by their surface density in the fusion products. Thus, fusion products consisting of a single virus particle and an increasing number of liposomes are likely to gradually regain their capacity to fuse with virus particles. On the other hand, it is conceivable that a decreasing average surface density of viral spike glycoproteins in the fusion products will result in a lower activity of fusion between the fusion products and additional liposomes.

At pH 6.0, 60–75% of the virus particles are incapable of fusing with CL liposomes (Table III). The fusion kinetics could be best simulated (Figure 6) by assuming that both inactive and active virus particles bind to the liposomes with the same aggregation rate constant as that at pH 5.0. This indicates that the affinity of influenza virus for CL liposomes is relatively independent of the pH, consistent with the observation that even at neutral pH, binding of the virus to CL liposomes is essentially complete (unpublished results). With respect to the actual fusion reaction at pH 6.0, it is apparent that the active virus particles fuse more slowly than at pH 5.0 (Table IV, Figure 6).

It is well established that the fusion activity of influenza virus is mediated by one of the spike glycoproteins, the hemagglutinin (HA) (White et al., 1982b, 1983). In its active form, the HA consists of two subunits HA_1 and HA_2. At the N-terminus, HA_2 contains an unusually hydrophobic sequence of amino acid residues, interrupted by three acidic amino acid residues (Min Jou et al., 1980; Gething et al., 1980; Richardson et al., 1980; Wilson et al., 1981). This hydrophobic segment becomes exposed by a low pH induced, irreversible, conformational change in the protein (Skehel et al., 1982; Yewdell et al., 1983) and is thought to be intimately involved in the fusion reaction, possibly by penetrating into the target membrane (White et al., 1983; Maeda et al., 1981; Sato et al., 1983). Recently, Doms et al., (1985) have studied in detail the pH dependence of the conformational change in the HA protein, using the water-soluble ectodomain of the molecule isolated from the virus by digestion with bromelain. After conversion to the acid form, the bromelain-solubilized fragment (BHA) binds to liposomes and becomes sensitive to proteinase K (Doms et al., 1985). It was demonstrated that the pH dependence of the conversion of BHA to the acid form was wider and shifted to slightly higher pH values than the pH dependence of the cell–cell fusion activity of the virus. This suggests that for virus-induced cell–cell fusion to occur the

cooperative action of more than a single HA molecule is required (Doms et al., 1985). From our present and previous work (Stegmann et al., 1985), it appears that the pH dependence of the fusion activity of the virus toward CL liposomes resembles more closely that of the conversion of BHA to the acid form than that of the cell–cell fusion activity of the virus. This indicates that in the system involving CL liposomes as target vesicles a cooperative action of acid-activated HA molecules may not be required. Thus, the relatively high residual fusion activity at pH 6.0 (Tables III and IV, Figure 6) is unlikely to be a precise reflection of the biological fusion activity of the virus. Rather, it appears the result of the use of negatively charged liposomes as target vesicles. In this respect it should be noted that fusion of the same strain of the virus with erythrocyte ghosts, monitored with a novel fluorescent assay (Hoekstra et al., 1984), as well as the hemolytic activity of the virus, displays a much steeper pH dependence than that of the fusion with CL liposomes: both fusion with erythrocyte ghosts and hemolysis are negligible at pH 6.0 (unpublished results).

From the above considerations it is apparent that for the initial adhesion of the virus and for the subsequent fusion reaction the nature and composition of the target membrane system are of critical importance. Therefore, in future studies the composition of the target membrane vesicles must be varied so as to mimick as closely as possible the target membrane for the virus in biological systems. Incorporation of specific receptors for the virus in liposomes of different compositions as well as kinetic studies on fusion of the virus with biological membrane vesicles (Hoekstra et al., 1984) is of particular interest in this respect. The procedure presented in this paper opens the possibility to kinetically analyze the results of such studies and to discriminate between the initial adhesion of the virus particles to the target membrane and the subsequent fusion reaction.

ACKNOWLEDGMENTS

We thank Mrs. Sue Salomon for typing the manuscript, Drs. S. WellingWester and G. Welling (Department of Microbiology, University of Groningen) for their help in preparing the virus, Dr. J. C. de Jong (Rijksinstituut voor de Volksgezondheid, Bilthoven, The Netherlands) for providing the X-47 influenza strain, and Drs. A. Helenius, M. Kielian, and R. Doms (Yale University, New Haven, CT) and Dr. J. White (University of California, San Francisco, CA) for stimulating discussions.

APPENDIX

The notations have been introduced in eq 1–6, and analytical solutions obtained by applying certain approximations are given in eq 7–32. The general equations for the kinetics of virus–vesicle aggregation and fusion, including deaggregation processes, are given below:

$$\frac{dA(I,J)}{dt} = \sum_{I_1=0,J_1=0}^{I,J} A(I_1,J_1)A(I-I_1,J-J_1)(1/2)C_1 - A(I,J)\{\sum_{I_1=0,J_1=0}^{N_L-I,N_V-J} A(I_1,J_1)C_1 + \sum_{I_1=1,J_1=1}^{M_L,M_V} F(I_1,J_1)C_2 + \sum_{I_1=0,J_1=0,I_2=1,J_2=1}^{M_L-I,M_V-J,M_L,M_V} AF(I_1,J_1,I_2,J_2)C_3\} - A(I,J)\{f(I,J) + DK(I,J)D_1\} + \sum_{I_1=I,J_1=J}^{N_L,N_V} A(I_1,J_1)D_1(1 + \delta_{I_1,2I}\delta_{J_1,2J}) + \sum_{I_1=I,J_1=J,I_2=1,J_2=1}^{M_L,M_V,M_L,M_V} AF(I_1,J_1,I_2,J_2)D_2 \quad (A1)$$

Here N_L and N_V are the largest allowed numbers of vesicles and virus particles, respectively, in an aggregate A or in a fusion product, F, and M_L and M_V have the same meaning with regard to AF and FF. The symmetric function $DK(I,J)$ is a combinatorial factor that has been evaluated to take into account that deaggregation cannot result in final products consisting exclusively of several virus particles or vesicles. As an example, $DK(2,1) = 1$, $DK(3,1) = 1$, $DK(3,3) = 4$, and $DK(4,4) = 7$. The aggregation and deaggregation rate constants, C_i and D_i, can be further specified as in Bentz et al. (1983a), but at this stage it seems preferable to keep the number of parameters at a minimum.

The δ functions have the usual meaning, being equal to 0 or 1. In all the terms, the program avoids processes that result in unallowed products such as $A(I,0)$, $F(I,0)$ where $I > 1$ or $A(0,J)$ where $J > 1$, etc. It may be noted that one of the indices I_1 or J_1 must be larger than the corresponding indices I or J, to allow for the deaggregation of $A(I_1,J_1)$ into $A(I,J)$.

$$\frac{dF(I,J)}{dt} = A(1,1)f(1,1)\delta_{I,1}\delta_{J,1} + f(I,J)\sum_{I_1=1,J_1=1}^{I-1,J-1} FF(I_1,J_1,I-I_1,J-J_1) + AF(1,0,I-1,J)f(I,J) + AF(0,1,I,J-1)f(I,J) - F(I,J)\{\sum_{I_1=0,J_1=0}^{M_L,M_V} A(I_1,J_1)C_2 + \sum_{I_1=1,J_1=1}^{M_L,M_V} F(I_1,J_1)C_4\} + \sum_{I_1=0,J_1=0}^{M_L,M_V} AF(I_1,J_1,I,J)D_2 + \sum_{I_1=1,J_1=1}^{M_L,M_V} \{FF(I,J,I_1,J_1) + FF(I_1,J_1,I,J)\}D_2 \quad (A2)$$

$$\frac{dAF(I_1,J_1,I_2,J_2)}{dt} = A(I_1,J_1)F(I_2,J_2)C_2 + \sum_{I_3=0,J_3=0}^{I_1,J_1} AF(I_1-I_3,J_1-J_3,I_2,J_2)A(I_3,J_3)C_3 + A(I_1+1,J_1+1)\bar{f}(1,1)\delta_{I_2,1}\delta_{J_2,1} + AF(I_1+1,J_1,I_2-1,J_2)\bar{f}(I_2,J_2) + AF(I_1,J_1+1,I_2,J_2-1)\bar{f}(I_2,J_2) - \sum_{I=0,J=0}^{M_L-I_1,M_V-J_1} AF(I_1,J_1,I_2,J_2)A(I,J)C_3 - AF(I_1,J_1,I_2,J_2)\bar{f}(I_1+I_2,J_1+J_2)(nf) - AF(I_1,J_1,I_2,J_2)D_2R(I_1,J_1) + \sum_{I=I_1,J=J_1}^{M_L,M_V} AF(I,J,I_2,J_2)D_2 \quad (A3)$$

In the last term in the summation, I or J must be larger than I_1 and J_1, respectively. The function $R(I_1,J_1)$ is a combinatorial factor slightly different from $DK(I_1,J_1)$, the difference arising from the fact that a term such as $AF(2,0,I_2,J_2)$ is allowed, whereas $A(2,0)$ is not allowed. In comparison, $R(2,1) = 4$ whereas $DK(2,1) = 1$. The integer nf can vary from 0 to 3, depending on the particular case. This factor accounts for the number of different fusion products formed from $AF(I_1,J_1,I_2,J_2)$. For instance, $AF(1,1,1,1)$ can transform via fusion into $AF(0,1,2,1)$, $AF(1,0,1,2)$, and $FF(1,1,1,1)$, so that in this case $nf = 3$; $AF(0,1,1,2)$ transforms via fusion into $F(1,3)$, i.e., nf = 1.

$$\frac{dFF(I_1,J_1,I_2,J_2)}{dt} = F(I_1,J_1)F(I_2,J_2)(1/2)C_2 + AF(1,1,I_2,J_2)f(I_2+1,J_2+1)\delta_{I_1,1}\delta_{J_1,1} - FF(I_1,J_1,I_2,J_2)f(I_1+I_2,J_1+J_2) - FF(I_1,J_1,I_2,J_2)D_2 \quad (A4)$$

The factor $^1/_2$ in eq A1 and A4 is introduced to preserve mass conservation for vesicles and virus particles. The expression of mass conservation for vesicles is

$$L_0 = \sum_{I,J} I\{A(I,J) + F(I,J)\} + \sum_{I_1,J_1,I_2,J_2} (I_1+I_2)\{AF(I_1,J_1,I_2,J_2) + FF(I_1,J_1,I_2,J_2)\} \quad \text{(A5)}$$

in which L_0 is initial concentration of vesicles. A similar equation holds for V_0. Since L_0 is a constant, the derivative of both sides of eq A5 must be indentically zero. The solution was obtained by a Taylor series expansion up to four terms, i.e.

$$y(t+h) = y(t) + hy(t) + (h^2/2)y''(t) + (h^3/6)y'''(t) \quad \text{(A6)}$$

where the function y is any one of the functions $A(I,J)$, $F(I,J)$, $AF(I_1,J_1,I_2,J_2)$, or $FF(I_1,J_1,I_2,J_2)$. At $t = 0$, $L_0 = A(1,0)$, $V_0 = A(0,1)$, and all the other functions are equal to zero. Equations A1–A4 provide the first derivatives, and both second and third derivatives are successively obtained. At this stage, eq A6 provides the values of the functions at time $t + h$ (i.e., at $t = h$ in the first step). The step h is chosen such that the desired accuracy is ensured. We employed several tests for the accuracy of the equations and the numerical solutions. One test was mass conservation for both vesicles and virus particles (see eq A5).

A very useful test was vanishing of the derivatives with respect to time of eq A5 or the analogous equation for V_0. The use of these tests on the derivatives facilitated the location of errors in the equations or in the program. A useful procedure was to set some of the rate constants to zero in the preliminary tests of the equations and program. Another criterion for accuracy was the ratio between the first derivatives of the functions with respect to h according to eq A6 or according to eq A1–A4. In practice, in most of the calculations, N_L and N_V were set equal to 4, which means that aggregation-fusion products could include up to eight particles. Doubling of this order did not result in meaningful changes in the results. Occasionally, numerical solutions could be compared with the results of analytical solutions.

The calculation of the percent increase in N-NBD-PE fluorescence (% Fl) utilizes eq 33. The contributions to % Fl arise from fused structures only, i.e., terms such as F, AF, and FF. The contribution of terms such as $F(I,J)$ to % Fl is given by $(100/L_0)[1 - I/(I + J)]IF(I,J)$ or $(100/L_0)F(I,J)IJ/(I + J)$. Hence

$$\% \text{ Fl} = (100/L_0)\{\sum_{I,J} F(I,J)IJ/(I + J) + \sum_{I_1,J_1,I_2,J_2} [J_2R_2AF(I_1,J_1,I_2,J_2) + (J_1R_1 + J_2R_2)FF(I_1,J_1,I_2,J_2)]\} \quad \text{(A7)}$$

in which $R_1 = I_1/(I_1 + J_1)$ and $R_2 = I_2/(I_2 + J_2)$.

By utilizing eq A5, we can obtain another form

$$\% \text{ Fl} = (100/L_0) \times \{L_0 - \sum_{I,J}[IA(I,J) - I^2F(I,J)/(I + J)] - \sum_{I_1,J_1,I_2,J_2} [(I_1 + I_2R_2)AF(I_1,J_1,I_2,J_2) + (I_1R_1 + I_2R_2)FF(I_1,J_1,I_2,J_2)]\} \quad \text{(A8)}$$

The program was written in BASIC for both APPLE and VAX computers.

References

Bartlett, G. R. (1959) *J. Biol. Chem. 234*, 466–468.

Bentz, J., Nir, S., & Wilschut, J. (1983a) *Colloids Surf. 6*, 333–363.

Bentz, J., Düzgünes, N., & Nir, S. (1983b) *Biochemistry 22*, 3320–3330.

Carroll, S. M., Higa, H. H., & Paulson, J. C. (1981) *J. Biol. Chem. 256*, 8357–8363.

Doms, R. W., Helenius, A., & White, J. (1985) *J. Biol. Chem. 260*, 2973–2981.

Driessen, A. J. M., Hoekstra, D., Scherphof, G., Kalicharan, R. D., & Wilschut, J. (1985) *J. Biol. Chem. 260*, 10880–10887.

Eidelman, O., Schlegel, R., Tralka, T. S., & Blumenthal, R. (1984) *J. Biol. Chem. 259*, 4622–4628.

Folch, J., Lees, M., & Sloane-Stanley, G. H. (1957) *J. Biol. Chem. 226*, 497–509.

Gething, M. J., Bye, J., Skehel, J., & Waterfield, M. (1980) *Nature (London) 287*, 301–306.

Helenius, A., Marsh, M., & White, J. (1980) *Trends Biochem. Sci. (Pers. Ed.) 5*, 104–106.

Helenius, A., Mellmann, I., Wall, D., & Hubbard, A. (1983) *Trends Biochem. Sci. (Pers. Ed.) 8*, 245–250.

Hoekstra, D. (1982) *Biochemistry 21*, 2833–2840.

Hoekstra, D., De Boer, T., Klappe, K., & Wilschut, J. (1984) *Biochemistry 23*, 5675–5681.

Kumar, N., Blumenthal, R., Henkart, M., Weinstein, J. N., & Klausner, R. D. (1982) *J. Biol. Chem. 257*, 15137–15144.

Maeda, T., Kawasaki, K., & Ohnishi, S. I. (1981) *Proc. Natl. Acad. Sci. U.S.A. 78*, 4133–4137.

Marsh, M., Bolzau, E., & Helenius, A. (1983) *Cell (Cambridge, Mass.) 32*, 931–940.

Matlin, K. S., Reggio, H., Helenius, A., & Simons, K. (1981) *J. Cell Biol. 91*, 601–613.

Min Jou, M., Verhoeyen, M., Devos, R., Samon, E., Fang, R., Huylebroeck, D., Friers, W., Threlfall, G., Barber, G., Carey, N., & Emtage, S. (1980) *Cell (Cambridge, Mass.) 19*, 683–696.

Nichols, J. W., & Pagano, R. E. (1983) *J. Biol. Chem. 258*, 5368–5371.

Nir, S., Bentz, J., & Wilschut, J. (1980a) *Biochemistry 19*, 6030–6036.

Nir, S., Bentz, J., & Portis, A. (1980b) *Adv. Chem. Ser. No. 188*, 75–106.

Nir, S., Wilschut, J., & Bentz, J. (1982) *Biochim. Biophys. Acta 688*, 275–278.

Nir, S., Bentz, J., Wilschut, J., & Düzgünes, N. (1983) *Prog. Surf. Sci. 13*, 1–124.

Olson, F., Hunt, C. A., Szoka, F. C., Vail, W. J., & Papahadjopoulos, D. (1979) *Biochim. Biophys. Acta 557*, 9–23.

Richardson, C. D., Scheid, A., & Choppin, P. W. (1980) *Virology 105*, 205–222.

Rogers, G. N., Paulson, J. C., Daniels, R. S., Skehel, J. J., Wilson, I. A., & Wiley, D. C. (1983a) *Nature (London) 304*, 76–78.

Rogers, G. N., Pritchett, T. J., Lane, J. L., & Paulson, J. C. (1983b) *Virology 131*, 394–408.

Rosenberg, J., Düzgünes, N., & Kayalar, C. (1983) *Biochim. Biophys. Acta 735*, 173–180.

Sato, S. B., Kawasaki, K., & Ohnishi, S. I. (1983) *Proc. Natl. Acad. Sci. U.S.A. 80*, 3153–3157.

Skehel, J. J., Bayley, P. M., Brown, E. B., Martin, S. R., Waterfield, M. B., White, J. M., Wilson, I. A., & Wiley, D. C. (1982) *Proc. Natl. Acad. Sci. U.S.A. 79*, 968–972.

Smoluchowski, M. (1917) *Z. Phys. Chem., Abt. A 92*, 129–168.

Stegmann, T., Hoekstra, D., Scherphof, G., & Wilschut, J. (1985) *Biochemistry 24*, 3107–3113.

Struck, D. K., Hoekstra, D., & Pagano, R. E. (1981) *Biochemistry 20*, 4093-4099.
Tycko, B., & Maxfield, F. R. (1982) *Cell (Cambridge, Mass.) 28*, 643-651.
Van Renswoude, J., Bridges, K. R., Harford, J. B., & Klausner, R. D. (1982) *Proc. Natl. Acad. Sci. U.S.A. 79*, 6186-6190.
White, J., & Helenius, A. (1980) *Proc. Natl. Acad. Sci. U.S.A. 77*, 3273-3277.
White, J., Helenius, A., & Kartenbeck, J. (1982a) *EMBO J. 1*, 217-222.
White, J., Helenius, A., & Gething, M. J. (1982b) *Nature (London) 300*, 658-659.
White, J., Kielian, M., & Helenius, A. (1983) *Q. Rev. Biophys. 16*, 151-195.
Wilschut, J., Düzgünes, N., Fraley, R., & Papahadjopoulos, D. (1980) *Biochemistry 19*, 6011-6021.
Wilschut, J., Nir, S., Scholma, J., & Hoekstra, D. (1985) *Biochemistry 24*, 4630-4636.
Wilson, I. A., Skehel, J. J., & Wiley, D. C. (1981) *Nature (London) 289*, 366-373.
Yewdell, J. W., Gerhard, W., & Bach, T. (1983) *J. Virol. 48*, 239-248.
Yoshimura, A., Kuroda, K., Kawasaki, K., Yamashina, S., Maeda, T., & Ohnishi, S. I. (1982) *J. Virol. 43*, 284-293.

Turn Prediction in Proteins Using a Pattern-Matching Approach†

F. E. Cohen,‡ R. M. Abarbanel,§,‖ I. D. Kuntz,*,‡ and R. J. Fletterick⊥
Departments of Pharmaceutical Chemistry, Medical Information Science, and Biochemistry, University of California at San Francisco, San Francisco, California 94143
Received May 2, 1985; Revised Manuscript Received August 20, 1985

ABSTRACT: We extend the use of amino acid sequence patterns [Cohen, F. E., Abarbanel, R. M., Kuntz, I. D., & Fletterick, R. J. (1983) *Biochemistry 22*, 4894-4904] to the identification of turns in globular proteins. The approach uses a conservative strategy, combined with a hierarchical search (strongest patterns first) and length-dependent masking, to achieve high accuracy (95%) on a test set of proteins of known structure. Applying the same procedure to homologous families gives a 90% success rate. Straightforward changes are suggested to improve the predictive power. The computer program, written in Lisp, provides a general pattern-recognition language well suited for a number of investigations of protein and nucleic acid sequences.

The recognition by Anfinsen et al. (1961) that amino acid sequence determines protein structure initiated a search for algorithms to predict protein tertiary structure from primary sequence. Two basic theoretical approaches to this problem have developed: energy minimization and semiempirical hierarchical condensation models. Energy calculations offer the advantage of a chemically plausible approach to structure prediction. This method is limited by difficulties in producing adequate energy functions and by problems with convergence [e.g., Momany et al. (1975), Levitt (1976), and Robson & Osguthorpe (1979)]. The semiempirical hierarchical condensation model assumes that the folding problem can be divided into a series of smaller problems. Traditional divisions have been the prediction of secondary structure from sequence [e.g., Chou & Fasman (1974), Lim (1974), Garnier et al. (1978), Taylor & Thornton (1983), and Cohen et al. (1983)], the prediction of approximate tertiary structure from secondary structure (Cohen et al., 1979, 1980, 1982; Ptitsyn & Rashin, 1975), and the refinement of approximate tertiary structure.

In a previous paper, we showed that the successful location of turns facilitated secondary structure assignment for the class of proteins that are formed from a β sheet surrounded by α helices (Cohen et al., 1983). This paper describes a more general approach to the location of turns in proteins of all three major classes of globular proteins: α/α, α/β, and β/β (Levitt & Chothia, 1976). The new algorithms make use of many of the tools of artificial intelligence "expert systems" (Barr & Feigenbaum, 1981) described in our earlier paper. A major advance is the creation of a pattern-matching language, Pattern Language for Amino and Nucleic Acid Sequences (PLANS), written in Lisp. Other computer languages could be employed, but Lisp appears best suited for further development. These algorithms accurately (>90%) locate turns in a large set of proteins. The complete set of patterns and an interpretation guide are presented in this report. Knowledge of turn location is of interest to biochemists and immunologists as a guide to structural or biochemical properties of proteins. Further, we expect that the new programs will ultimately lead to a reasonable, complete, and accurate method of secondary structure prediction.

Theory and Methods

We will consider a subset of globular proteins that consist of one or more sequentially contiguous domains where each domain is a member of one of three classes of protein structure: α/α, α/β, or β/β. The proteins of interest include at least half of the known structures. We treat the protein backbone as a series of regular helical and/or strand conformations connected by turns. Turns for our purposes are defined as regions of the chain between regular secondary structure elements; they may be from two to more than fifteen amino acids in length. They are frequently made from amino acids that are relatively accessible to solvent and hydrophilic in character. These assumptions constitute a simple model for domains in globular proteins.

A *hierarchical* approach is used in the algorithms we use to find turns. We wish to avoid the difficulties associated with "cutoff" or "threshold" parameters. Intuition and experience

† This research was supported by Grants 5R23LM03893 (R.M.A.), GM34197 (I.D.K.), and AM26081 (R.J.F.).
‡ Department of Pharmaceutical Chemistry.
§ Department of Medical Information Science.
‖ Present address: Intellicorp, Mountain View, CA 94040.
⊥ Department of Biochemistry.

0006-2960/86/0425-0266$01.50/0